

Vibrational Relaxation of Carbon Monoxide Studied by Two-Wavelength Infrared Emission

CHARLES CHACKERIAN Jr.*

NASA Ames Research Center, Moffett Field, Calif.

Experimental results are presented for the vibrational relaxation of pure carbon monoxide behind incident shock waves over the temperature range 4000°K to 6300°K. The data were obtained as infrared emission from the fundamental and overtone vibrational band systems (in some of the experiments the two-band systems were recorded simultaneously). The data are consistent with present theories for the vibrational relaxation of diatomic molecules and can be interpreted in terms of an initial Boltzmann vibrational distribution relaxing toward final equilibrium via a continuous sequence of intermediate Boltzmann distributions.

Introduction

THE literature is replete with shock-wave studies of vibrational relaxation using a number of experimental techniques, and in general good correlation¹ has been obtained, over large ranges of temperature, between experimental data and the Landau-Teller theory² which relates the characteristic vibrational relaxation time to the gas-kinetic temperature. In particular, for carbon monoxide, spectroscopic techniques (infrared emission and sodium line reversal) have been used³⁻⁵ to yield vibrational relaxation data up to about 3000°K; Matthews⁶ obtained relaxation data behind incident shocks between 2200°K and 4900°K using interferometry, and in addition, Hanson⁷ has made measurements between 2400°K and 6000°K using end-wall pressure measurements. The vibrational relaxation of carbon monoxide has also been studied in expanding flows^{8,9} with stagnation temperatures ranging between 1200°K and 5200°K. The results of the expansion experiments are in conflict with shock-wave results. Some experimenters have found that vibrational de-excitation appears to occur at a rate faster than would be calculated from vibrational excitation rates. Theoretical arguments based on molecular anharmonicity have been advanced by Bray¹⁰ to explain this apparent discrepancy. On the other hand, other experimenters⁹ have not observed such an effect and suggest the possible effect of impurities or improper interpretation of the data to be the source of the discrepancy. The data of this investigation are somewhat complementary to the expansion studies in that very high vibrational temperatures are obtained. However, unlike the expansion work, the translation temperature is also very high such that the large discrepancy in magnitude between the *V-V* (vibrational-vibration) and *V-T* (vibration-translation) energy transfer cross sections (theoretical) does not exist as it does in the expansion studies.

Data for this work were obtained as infrared emission records. The present study can be distinguished from the previous studies employing spectroscopic techniques cited previously³⁻⁵ in the following respects: a) the translational temperature range has been extended (4000°-6300°K); b) infrared emission records were obtained simultaneously from the fundamental and overtone vibrational band systems; and c) theory and experiment were compared on the entire relaxation profile rather than at a single characteristic time. The significance of the simultaneous measurement of the fundamental and overtone band systems is

that the infrared emission from these two systems has a different functional dependence on the vibrational temperature so that within experimental error the measurements provide a stringent test of the theoretical model for the relaxation process.

Experimental

The experimental data consist either of emission records of the vibrational fundamental or of emission records obtained simultaneously of the fundamental and overtone bands of carbon monoxide heated behind incident shock waves. The detection system, which was located about 35 ft from the diaphragm, is shown in Fig. 1. The radiation passed through a window (50.8 mm in height), mounted in a boundary-layer splitter plate, and through two 1-mm-wide collimating slits. The optical path external to the shock tube was flushed with dry nitrogen to reduce the possibility of atmospheric absorption. A similar splitter plate on the opposite wall of the shock tube defined a 229-mm optical path in the shock tube, and the spatial resolution of the optical system at the position of this splitter plate was about 3 mm. Any advantage of using splitter plates over looking through the side-wall boundary layer was not established experimentally, but it was felt that looking through the constant boundary layer (steady state) afforded by the splitter plate¹⁴ would be advantageous over looking through the constantly increasing boundary layer on the side wall.

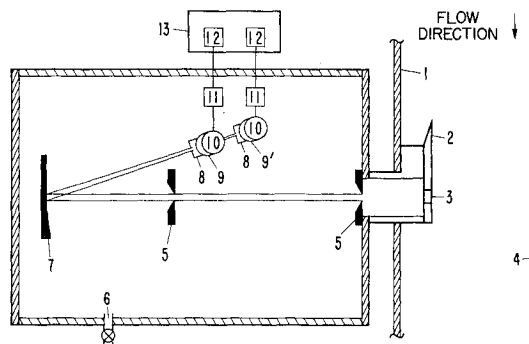


Fig. 1 Schematic of infrared detection system. 1) Shock tube wall; 2) boundary-layer splitter plate; 3) CaF_2 window; 4) shock-tube center line; 5) collimating slits; 6) dry gas inlet; 7) off-axis parabolic mirror; 8) turning mirrors; 9) interference filters; 10) indium antimonide detectors; 11) preamplifiers; 12) and 13) recording oscilloscope and amplifier.

Received February 14, 1973; revision received July 16, 1973. The author wishes to acknowledge many helpful discussions with L. Presley, P. Rowley and M. Rubesin, and the technical assistance of W. Hackett.

Index category: Shock Waves and Detonations.

* Research Scientist, Astrophysics Branch, Space Science Division.

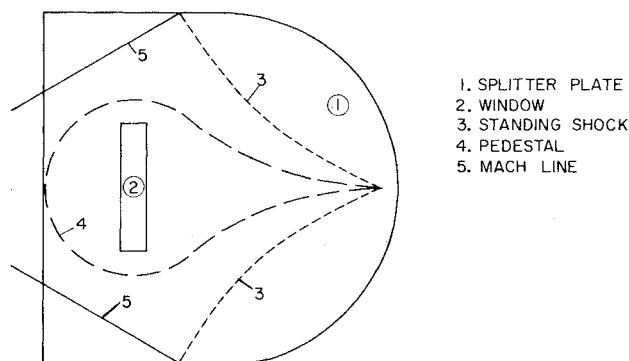


Fig. 2 Planview of boundary-layer splitter plate and pedestal.

A plan diagram for the boundary-layer splitter plate and its pedestal is shown in Fig. 2. The pedestal was designed such that the region of influence of the standing shock (formed by the pedestal) above the splitter plate did not extend into the line of sight of the infrared detectors. The positions of the standing shock and Mach line ($M_1 = 10$) above the splitter plate are also shown on Fig. 2. The positions of standing shocks formed by the pedestal were determined experimentally from photographs of the visible light emission from the standing shock with the splitter plate removed. It is also possible that deceleration of the shock wave on the splitter plate could influence data near the shock front (first three or four μsec), but if this deceleration is typical of the side wall value, this effect should be negligible.

Shock velocities were determined by using piezoelectric gauges and submicrosecond counters; the shocks were found to decelerate at a negligible rate (about $0.05 \text{ mm}/\mu\text{sec-m}$). The relative response of the filter-detector combination as well as vibrational band center positions are shown in Fig. 3. The relative response with wavelength of the indium antimonide detectors was determined by comparison with a gold thermocouple which is known to have flat response out to 6μ .

The 12-in.-diam arc-driven shock tube used for the present study has been described by Presley et al.¹¹ The gas impurity level determined by the outgassing rate ranged from about 0.5 to $1 \mu\text{Hg}$; the initial CO pressures were from 380 to $790 \mu\text{Hg}$ (impurities mostly H_2O and N_2 in about equal amounts were identified by their mass spectra). An upper limit of 4% was calculated for the effect water vapor can have in accelerating the vibrational relaxation time of carbon monoxide at 4000°K using data obtained by von Rosenberg Jr. et al.¹² The upper limit was calculated assuming a 0.1% water impurity level, and

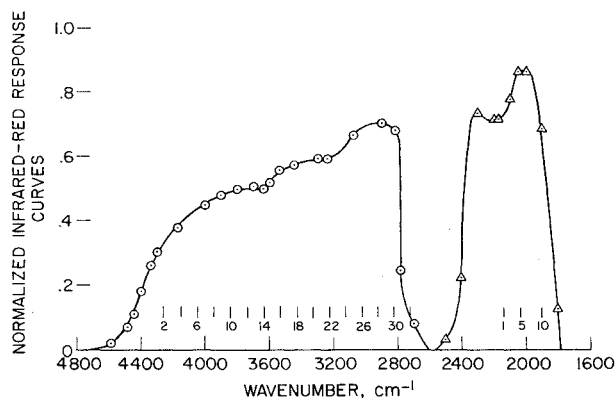


Fig. 3 Relative infrared filter-detector response curves (FD): Δ , fundamental; \odot , overtone; vibrational band centers indicated by tick marks. Transmission of the filters beyond the ranges indicated in the figure is less than 0.1%.

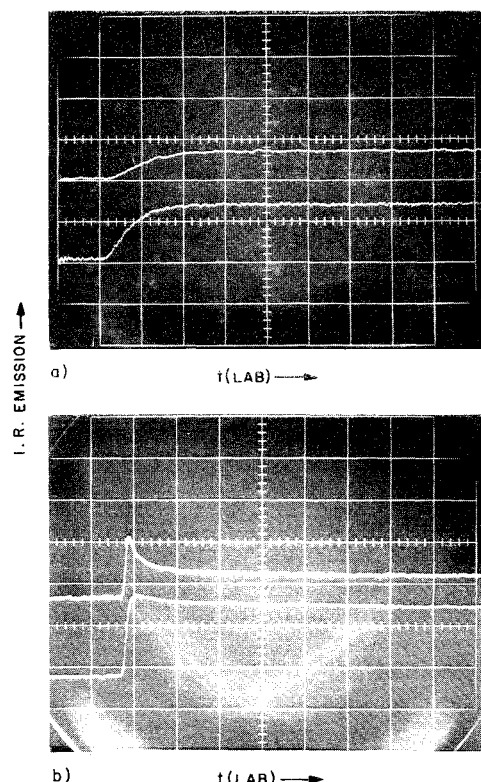


Fig. 4 Two wavelength infrared emission traces. Upper trace in each panel is the overtone signal (O), lower trace, the fundamental (F); sweep is $5 \mu\text{s/cm}$. a) $U_1 = 3.48 \text{ km/sec}$, $P_1 = 0.49 \text{ torr}$; b) $U_1 = 5.63 \text{ km/sec}$, $P_1 = 0.3 \text{ torr}$. The electronic risetimes of the two channels are the same but the overtone emission signal peaks sooner than the fundamental mainly because it exhibits a larger nonequilibrium overshoot. In this case considerable dissociation occurs.

the systematics of vibrational relaxation discussed by Millikan and White¹ was used to extrapolate von Rosenberg's data from 2600°K to 4000°K . Photographically recorded spectra of the shocked gas indicated the presence of small amounts of C_2 , CN, Al and Na.

Data Reduction

Typical oscilloscope emission records of weak and strong shocks are shown in Figs. 4a and 4b, respectively. The coincidence in time of the initial rise of the traces in Fig. 4b (here the vibrational relaxation time is approximately $1 \mu\text{sec}$) indicates that the optical path for the two detectors is spatially coaligned in the plane perpendicular to the shock-tube axis. The combined effects of electronics, shock-wave curvature, and finite spatial resolution of the infrared detection system cause the infrared emission profile to be distorted near the shock front and to be uniformly delayed in time (but not distorted) for times greater than about $1 \mu\text{sec}$. The zero of time on the experimental traces was chosen by extrapolating linearly the fundamental emission in the vicinity beyond about $1 \mu\text{sec}$ down to the zero intensity level; the same position on the oscilloscope trace abscissa was chosen as the zero of time for the overtone profiles. (This procedure was justified by calculations based on Appendices A and B.) The oscilloscope records were read with a telereader and were normalized by the emission intensity at equilibrium.

Calculations

Normal Shock

A normal shock computer program¹³ employing the usual flux

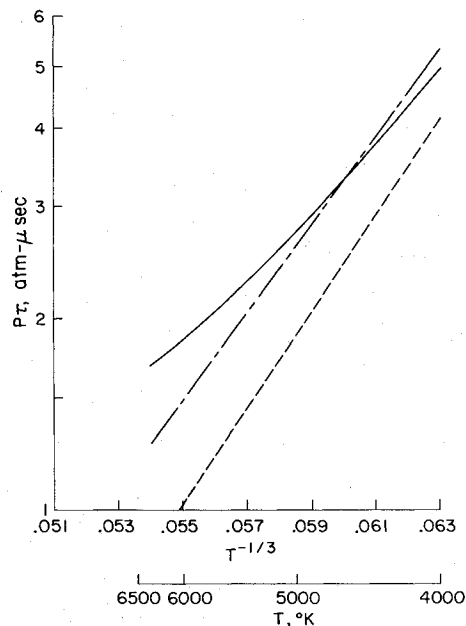


Fig. 5 Landau-Teller plot —, present data; ---, Hooker and Millikan; - · - · -, Matthews, Hanson.

conservation equations was used to obtain the vibrational temperature at points through the shock assuming a Boltzmann harmonic-oscillator vibrational distribution at each point. The Bethe-Teller equation [Eq. (1)] for the relaxation of vibrational energy, $E_v(T)$, was assumed to hold for each interval of the integration.

$$E_v(T) = [E_v(T_\infty) - E_v(T)]/\tau(T) \quad (1)$$

with the vibrational relaxation time, $\tau(T)$, at the local translational temperature, T , given by

$$P\tau(T) = \frac{(4.82 \times 10^{-10}) T^{5/6} \exp(238/T^{1/3})}{\Omega^{(2.2)*}(T)[1 - \exp(-3084/T)]} \text{ atm-}\mu\text{sec} \quad (2)$$

where

$$\Omega^{(2.2)*} = 0.877 - 0.72 \times 10^{-4}(T) + 0.606 \times 10^{-8}(T^2) - 0.16610^{-12}(T^3)$$

Equation (2) gives a best fit to the present data. A Landau-Teller plot of Eq. (2) is presented in Fig. 5. The resulting curve is in reasonably good agreement with the extrapolation to higher temperatures of results obtained by Hooker and Millikan⁴ between 1100 and 2500°K. The curve is also in reasonable agreement with results obtained by Matthews and Hanson⁷ over a temperature range similar to that of this work. The source of the discrepancy in Fig. 5 is not understood. The effect which gas impurities can have in shortening vibrational relaxation times diminishes with increasing temperature; the discrepancy between the data, however, increases with temperature.

Infrared Intensities

The infrared fundamental I_f and overtone I_o emission intensities (at the laboratory time, t) were evaluated via the following:

$$I_f(t) \propto \rho(t) \sum_{V=0}^{15} (V) N_v(t) \cdot FD_f(V) \cdot A(V, 1) \cdot W_f(V) \quad (3)$$

$$I_o(t) \propto \rho(t) \sum_{V=0}^{30} (V)(V-1) \cdot N_v(t) \cdot FD_o(V) \cdot A(V, 2) \cdot W_o(V) \quad (4)$$

where ρ is the gas density, V is the vibrational quantum number, $FD(V)$ the relative filter-detector response evaluated at the V vibrational band center (see Fig. 3), A corrects the intensities for vibrational anharmonicity,¹⁴ and the $W_i(V)$

represent the cube of the vibrational transition frequency (cm^{-1}) evaluated at the appropriate vibrational band center. Limits on the summations are determined by the filter-detector combination response shown in Fig. 3. The CO fractional vibrational level populations, $N_v(t)$, at a particular laboratory time, t , were obtained from the local vibrational temperature (T_v) calculated by the normal shock computer program, referenced above, via the Boltzmann function

$$N_v(t) = N_v(T_v) = \frac{\exp\{-3125.1[V - 0.00628(V^2 + V)]/T_v\}}{Z(T_v)} \quad (5)$$

where $Z(T_v)$ is the vibrational partition function. For the purpose of comparison with the experimental data the theoretical intensities were normalized by the appropriate equilibrium value.

Nonideal Effects

A number of possible nonideal effects were considered and the following were found to be negligible: 1) shock-wave deceleration, 2) absorption of radiation by the cold splitter-plate boundary layer, 3) self-absorption of the emitted radiation (checked experimentally), and 4) enhancement of the infrared emission signal from impurity CN molecules (the concentration of CN molecules was judged to be small as estimated from the intensity of time integrated spectra of the CN violet bands). For typical conditions of these experiments the splitter-plate boundary layer (at the position of the observation window, 30 μsec after arrival of the shock) can be approximated as having an optical depth of $2 \times 10^{-3} \text{ cm-atm}$ at 300°K. Assuming an average value for the absorption coefficient of $1.6 \text{ cm}^{-1} \text{ atm}^{-1}$ the absorption then is negligible.¹⁵

Bremsstrahlung radiation and side-wall boundary-layer corrections may be important but have not been included quantitatively in the interpretation of the data. The contribution of bremsstrahlung radiation to the infrared emission will be most important in the overtone spectral region. A crude estimate of this using bremsstrahlung data for nitrogen¹⁶ and infrared emission calculations¹⁷ leads to a possible enhancement of the infrared signal of 5% at equilibrium at 6500°K. Mirels¹⁸ has discussed the effect the side-wall boundary layer has in producing axial gradients in the core fluid properties of the shock. The most important corrections should be made to the time of flight and temperature and in the least favorable cases (lowest initial pressures) these parameters should each be increased by about 5% at equilibrium. The effects which some of the above corrections could have on the interpretation of the data are discussed below.

Results

Figure 6 is a comparison between the theoretical and experimentally obtained normalized infrared intensities in a run in

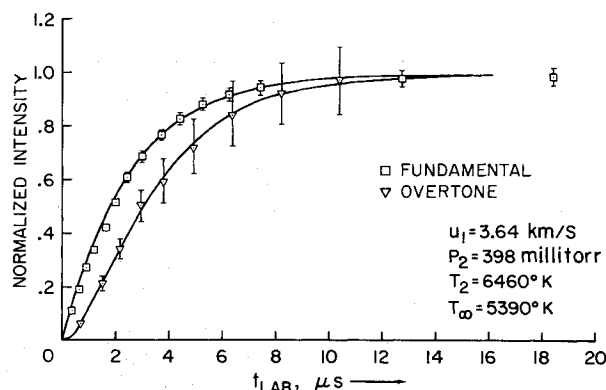


Fig. 6 Comparison between theory and experiment of normalized infrared intensities.

which the fundamental and overtone data were obtained simultaneously. As can be seen there is excellent agreement between theory and experiment. The simultaneous agreement of the fundamental and overtone emission records with theory indicates that multiple quantum V - T processes (which would be most probable in the hottest region of the shock wave, near the shock front) do not occur to a measurable extent. Figure 7 is a comparison of theory and experiment for a number of experimental runs. For economy of presentation of the data the comparisons are done as plots of vibrational temperature vs the theoretical translational temperature, where the theoretical translational temperature can be thought of as parameterizing laboratory time. Previous workers^{6,19,20} have elected to compare theory and experiment on a Landau-Teller plot ($P\tau$ vs $T^{-1/3}$) which, however, requires taking the slope of the data at points through the relaxation profile. This method of analysis can be subject to large errors in the near equilibrium region of the shock profile. Vibrational temperature profiles were obtained from normalized plots of the emission data (e.g., $I_f(t)/I_f(\infty)$ vs t) via the normalized form of Eqs. (3) or (4) assuming that $N_v(t)$ is given by the Boltzmann equation, Eq. (5). The experimentally determined vibrational temperature at the laboratory time, t , was then plotted against the theoretical value for the translational temperature at the same laboratory time, t . If the experimentally determined vibrational temperature does not fall on the theoretical curve then the translational temperature it is plotted against does not represent the true translational temperature of the gas at time t in the experiment. However, the plot is a valid comparison of vibrational temperatures at nearly the correct translation temperature. The solid curves on Fig. 7 are plots of the theoretical values of vibrational temperature vs translational temperature. The plots start at vibrational temperatures greater than room temperature because data within the first μsec of the relaxation profiles were not considered valid as a result of the shock profile distortion discussed under Data Reduction. In theory, the error in the vibrational temperature measurements is determined by the signal-to-noise on the oscilloscope records and the accuracy of the shock front location. In practice, the shock front could be located with negligible error, and the error for the vibrational temperature measurements was determined as the limits $[I(t) \pm E]/[I(\infty) \mp E]$ (see Fig. 6) where E is the half-width of the noise trace. The possible experimental error indicated in the caption to Fig. 7 is

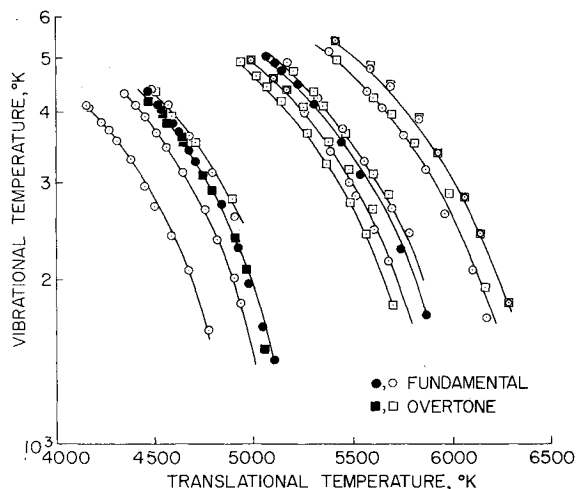


Fig. 7 Inferred vibrational temperature vs translational temperature, comparison between theory and experiment. The experimental uncertainty in vibrational temperature for the highest temperature run is: near equilibrium, ΔT_v (fundamental) = 120°K, ΔT_v (overtone) = 400°K; near the shock front, ΔT_v (fundamental) = 80°K, ΔT_v (overtone) = 280°K.

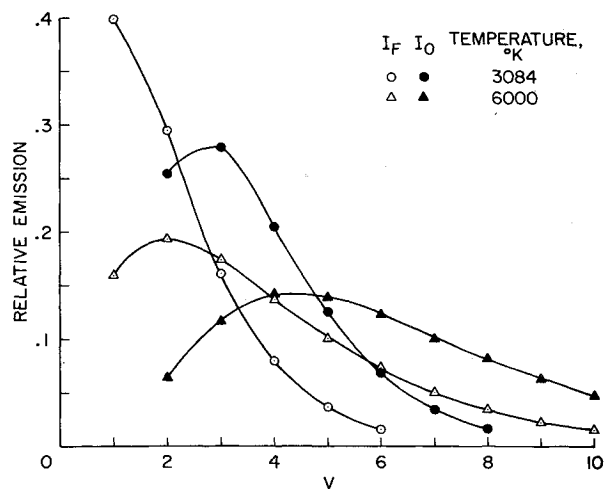


Fig. 8 Fractional contribution to infrared intensities as a function of vibrational quantum number, V .

for the run with the largest error; it is also the run which is plotted in Fig. 6. It can be seen from an examination of Fig. 7 that for translational temperatures below about 6000°K the agreement between the theoretical and experimentally derived vibrational temperatures is better than 100°K at all of the measured points as determined from either the fundamental or overtone band systems.

Discussion and Conclusions

C. C. Rankin and J. C. Light²¹ have obtained a solution to the master equation for a pure harmonic oscillator gas under the restriction that the selection rule for collisional vibrational transitions is $\Delta V = \pm 1$ (V - V and V - T processes allowed) and have obtained the result that an initial Boltzmann vibrational distribution relaxes to final equilibrium via a continuous sequence of intermediate Boltzmann distributions [it should be noted that Eq. (1) also results from the above model]. Bray²² studied the same problem, but allowed for vibrational anharmonicity; his results indicate that the effects of anharmonicity can be neglected for the purpose of the interpretation of these experiments. The temperature dependence of $P\tau$ [Eq. (2)] has been checked in a number of heat bath experiments in which characteristic vibrational relaxation times were determined. Recently, however, some pure gas studies^{6,19,20} done behind reflected shock waves have indicated that $P\tau$ should depend on the degree of vibrational excitation in such a way that $P\tau$ should be increasingly diminished over the value given by Eq. (2) as the degree of vibrational excitation is increased, and (as in the case of the expansion studies) it has been suggested that molecular anharmonicity could be responsible for the deviation between theory and experiment. This conclusion is not borne out by the data in Fig. 7, for initial shock temperatures less than 6300°K, because of very close agreement between the theoretical vibrational temperature profiles and those inferred from experiment. The results may not be inconsistent with those of Appleton,¹⁹ however, as the experimental data presented here are sensitive mainly to low vibrational levels (see Fig. 8) while Appleton based his conclusions on measurements characteristic of the tenth vibrational level in nitrogen. Deviations between theory and experiment for the stronger shocks (done at lower initial pressures) are of the same order as calculated from the boundary-layer correction discussed by Mirels¹⁸ and probably are not due to the effect discussed by Appleton.

Since the constants in Eqs. (3) and (4) have been well established by spectroscopic measurements it is concluded that the data presented herein constitute corroboration for the

theory of Rankin and Light for the lower levels of carbon monoxide up to 6300°K. The data are also not inconsistent with theory developed by Bray,²² which assumes a Treanor²³ vibrational distribution for the lower levels, since Bray has shown that the effects of anharmonicity are small for the conditions of these experiments.

Appendix A

An expression is obtained for the convolution of the effects of finite spatial resolution and shock curvature on the theoretical infrared (fundamental) emission profile behind the shock wave in order to establish the validity of the method used to determine the zero of time on the experimental traces. It was found that theoretical plots of the normalized infrared emission profile against laboratory time could be fit by Eq. (A1).

$$I_N^{-1}(t_L) = 1 - e^{-t_L/\tau} \quad (A1)$$

where $\tau = T_{1/2}/0.693$, and $T_{1/2}$ is the time required to attain half the equilibrium signal. The coordinate system used for the analysis of the problem is described by Wray.²⁴ The final expression for the "convoluted" normalized theoretical intensity ratio is given by Eq. (A2).

$$I_N^{-1} = \frac{\Delta(x'/\delta)^{1/2} - [\exp(-T/\tau)]K(x')[\exp(\Delta/U_s\tau) - 1]U_s\tau}{\Delta_\infty} \quad (A2)$$

where Δ_∞ is the spatial resolution of the optical system, Δ the length of hot gas "seen" by the detector, U_s the incident shock speed, and δ the shock curvature.²¹

$$K(x') = \left(\frac{U_s\tau}{\delta}\right)^{1/2} \int_0^{(x'/U_s\tau)^{1/2}} e^{t^2} dt \quad (A3)$$

For the calculations x' was increased stepwise until $x' = \delta$ and Δ increased until $\Delta = \Delta_\infty$; both were thereafter held constant at their respective limiting values. A more complicated expression is obtained for the normalized overtone intensity ratio by starting with the square of Eq. (A1). The shock wave curvature, δ , in the 1-ft-diam shock tube was obtained from the following: $\delta = (d^2)/(7.5 \times 10^4)(P_1)^{1/2}$ (mm), where d is the splitter-plate separation, and P_1 the upstream pressure. The appropriate constants in this equation were obtained by combining shock curvature data obtained in a 2-ft-diam tube by Lin and Fyfe²⁵ with a shock curvature equation: $\delta = k(R/P_1)^{1/2}$, where R is the tube radius and k a constant.

An equation appropriate for analysis of overtone data was obtained for the convolution of the square of Eq. (A1). It is similar to Eq. (A2) except that it contains in the numerator an additional term:

$$(-\tau/2)[(K/(2')^{1/2}x')/(2')^{1/2}][\exp-2(T+\Delta/U_s)/\tau - \exp-2T/\tau]$$

Appendix B

The electronic transfer function of the detection circuitry was assumed to be determined by the plug-ins (1A7A) used with the dual beam oscilloscope. Assume that the input can be described by Eq. (A1), then the output (assuming a transfer function characteristic of an RC-circuit, capacitance to ground) was determined from

$$E_o(t) = L^{-1}[(S\tau + 1)I_N'(S)] \quad (B1)$$

where L^{-1} indicates the inverse Laplace transform, and $\tau = 1/2\pi\omega_c$, where ω_c is the corner frequency on a diagram of the high frequency roll off of the amplifier.²⁶ Equation (B1) was used to test for distortion in assumed relaxation profiles and with the exception of a small uniform shift in the time domain, distortion of the fastest rising signals was found to be negligible for times greater than about 1 μ sec.

References

- 1 Millikan, R. C. and White, D. R., "Systematics of Vibrational Relaxation," *Journal of Chemical Physics*, Vol. 39, 1963, pp. 3209-3213.
- 2 Landau, L. and Teller, E., "Contribution to the Theory of Sound Dispersion," *Physikalische Zeitschrift der Sowjetunion*, Vol. 10, 1936, p. 34.
- 3 Davidson, N., "Measurement of the Vibrational Relaxation Time of CO Behind a Shock Wave by Infrared Emission," *Journal of Chemical Physics*, Vol. 27, 1957, p. 315.
- 4 Hooker, W. J. and Millikan, R. C., "Shock-Tube Study of Vibrational Relaxation in Carbon Monoxide for the Fundamental and First Overtone," *Journal of Chemical Physics*, Vol. 38, 1963, pp. 214-220.
- 5 Russo, A. L., "Spectrophotometric Measurements of the Vibrational Relaxation of CO in Shock-Wave and Nozzle Expansion-Flow Environments," *Journal of Chemical Physics*, Vol. 47, 1963, pp. 5201-5210.
- 6 Matthews, D. L., "Vibrational Relaxation of Carbon Monoxide in the Shock Tube," *Journal of Chemical Physics*, Vol. 34, 1961, pp. 639-642.
- 7 Hanson, R. K., "Shock-Tube Study of Vibrational Relaxation in Carbon Monoxide Using Pressure Measurements," *AIAA Journal*, Vol. 9, No. 9, Sept. 1971, pp. 1811-1819.
- 8 McLaren, T. I. and Appleton, J. P., "Vibrational Relaxation Measurements of Carbon Monoxide in a Shock-Tube Expansion Wave," *Journal of Chemical Physics*, Vol. 53, 1970, pp. 2850-2857.
- 9 Just, T. and Roth, P., "Measurements of CO Relaxation in an Unsteady Expansion Wave," *Journal of Chemical Physics*, Vol. 55, 1971, pp. 2395-2399.
- 10 Bray, K. N. C., "Vibrational Relaxation of Anharmonic Oscillator Molecules II Non-Isothermal Conditions," *Journal of Physics*, Vol. B3, 1970, pp. 1515-1538.
- 11 Presley, L. L. and Chackerian, C., Jr., "The Dissociation Rate of Carbon Monoxide Between 7,000°K and 15,000°K," AIAA Paper 66-518, New York, 1966.
- 12 von Rosenberg, E. W., Jr., Bray, K. N. C., and Pratt, N. H., "The Effect of Water Vapor on the Vibrational Relaxation of CO," *Thirteenth Symposium (International) on Combustion*, Combustion Institute Press, New York, 1970, pp. 89-98.
- 13 Marrone, P. V., "Inviscid Nonequilibrium Flow Behind Bow and Normal Shock Waves," QM-1626-A-12(I), May 1963, Cornell Aeronautical Lab., Buffalo, N.Y.
- 14 Chackerian, C., Jr., "Calculation of High-Temperature Steradiancy For Vibration-Rotation Bands of Carbon Monoxide," *Journal of Quantitative Spectroscopy and Radiative Transfer*, Vol. 10, 1970, pp. 271-282.
- 15 Cook, W., private communication, 1971, Iowa State Univ., Ames, Iowa.
- 16 Taylor, R. L., "Continuum Infrared Radiation from High-Temperature Air and Nitrogen," *Journal of Chemical Physics*, Vol. 39, 1963, pp. 2354-2360.
- 17 Young, L. A., "CO Infrared Spectra," *Journal of Quantitative Spectroscopy and Radiative Transfer*, Vol. 8, 1968, pp. 693-716.
- 18 Mirels, H., "Flow Nonuniformity in Shock Tubes Operating at Maximum Test Times," *Physics of Fluids*, Vol. 9, 1966, pp. 1907-1912.
- 19 Appleton, J. P., "Shock-Tube Study of the Vibrational Relaxation of Nitrogen Using Vacuum-Ultraviolet Light Absorption," *Journal of Chemical Physics*, Vol. 47, 1967, pp. 3231-3240.
- 20 Hanson, R. K. and Baganoff, D., "Shock-Tube Study of Vibrational Relaxation in Nitrogen Using Pressure Measurements," *Journal of Chemical Physics*, Vol. 53, 1970, pp. 4401-4403.
- 21 Rankin, C. C. and Light, J. C., "Relaxation of a Gas of Harmonic Oscillators," *Journal of Chemical Physics*, Vol. 46, 1967, pp. 1305-1316.
- 22 Bray, N. C., "Vibrational Relaxation of Anharmonic Oscillator Molecules," Fluid Mechanics Lab. Pub. 67-3, June 1967, MIT, Cambridge, Mass.
- 23 Treanor, C. E., Rich, J. W., and Rehm, R. G., "Vibrational Relaxation of Anharmonic Oscillators with Exchange-Dominated Collisions," *Journal of Chemical Physics*, Vol. 48, 1968, pp. 1798-1807.
- 24 Wray, K. L., "Shock-Tube Study of the Coupling of the O₂-Ar Rates of Dissociation and Vibrational Relaxation," *Journal of Chemical Physics*, Vol. 37, 1962, pp. 1254-1263.
- 25 Lin, S. C. and Fyfe, W. I., "Low-Density Shock Tube for Chemical Kinetics Studies," *Physics of Fluids*, Vol. 4, 1961, pp. 238-249.
- 26 Thaler, G. J. and Brown, R. G., *Analysis and Design of Feedback Control Systems*, McGraw-Hill, New York, 1960, pp. 118 and 175.